

Received:  
28 January 2016

Revised:  
4 May 2016

Accepted:  
12 May 2016

<http://dx.doi.org/10.1259/bjr.20160101>

Cite this article as:

Van Holsbeeck A, Degroote A, De Wever L, Vanhoutte E, De Keyzer F, Van Poppel H, et al. Staging of prostatic carcinoma at 1.5-T MRI: correlation of a simplified MRI exam with whole-mount radical prostatectomy specimens. *Br J Radiol* 2016; **89**: 20160101.

## FULL PAPER

# Staging of prostatic carcinoma at 1.5-T MRI: correlation of a simplified MRI exam with whole-mount radical prostatectomy specimens

<sup>1</sup>ANDRIES VAN HOLSBEECK, MD, <sup>2</sup>ANNEMARIE DEGROOTE, MD, <sup>1</sup>LIESBETH DE WEVER, MD, <sup>1</sup>ELS VANHOUTTE, MD, <sup>1</sup>FREDERIK DE KEYZER, MSc, <sup>3</sup>HENDRIK VAN POPPEL, PhD and <sup>1</sup>RAYMOND OYEN, PhD

<sup>1</sup>Department of Radiology, University Hospitals Leuven, Leuven, Belgium

<sup>2</sup>Department of Histopathology, University Hospitals Leuven, Leuven, Belgium

<sup>3</sup>Department of Urology, University Hospitals Leuven, Leuven, Belgium

Address correspondence to: Raymond Oyen

E-mail: [Raymond.oyen@uzleuven.be](mailto:Raymond.oyen@uzleuven.be)

**Objective:** To retrospectively analyze the accuracy of simplified multiparametric MRI at 1.5 T for local staging by using whole-mount-section histopathological analysis as the standard of reference.

**Methods:** 123 consecutive patients underwent  $T_2$  weighted,  $T_1$  weighted and diffusion-weighted MRI without endorectal coil prior to radical prostatectomy. The accuracy of predicting extracapsular extension (ECE) (T3a) was assessed using direct signs or the combination of direct and indirect signs of extraprostatic extension. The accuracy of predicting seminal vesicle invasion (T3b) was evaluated, taking into account different routes of seminal vesicle involvement. Finally, adjacent organ invasion (T4) was evaluated in this patient population.

**Results:** Histopathology showed T3a, T3b and T4 in 61, 28 and 9 cases, respectively. The use of direct signs of extraprostatic extension showed a sensitivity of 57.4% and

specificity of 91.9%. The combination of direct signs and indirect signs improved sensitivity (85.2%) at the expense of moderate loss of specificity (83.9%). MR sensitivity for the detection of seminal vesicle invasion was low (53.6%); however, it was dependent on the route of seminal vesicle tumour infiltration. MR sensitivity and specificity for adjacent organ invasion were 88.9% and 99.1%.

**Conclusion:** Simplified MRI study at 1.5 T provides a relatively high sensitivity for detecting ECE (T3a) when using the combination of indirect and direct signs. However, this high sensitivity reading is at the cost of a moderate loss of specificity. Invasion of the seminal vesicles (T3b) occurs most often along the ejaculatory duct complex with low MR sensitivity.

**Advances in knowledge:** Simplified MRI study at 1.5 T without endorectal coil could be used for the local T staging of prostate cancer.

## INTRODUCTION

Prostate cancer has become the leading cause of cancer worldwide in 2013 among males. The American Cancer Society estimated 220,800 new cases and 27,540 deaths related to prostate cancer among American males in 2015.<sup>1,2</sup>

Multiparametric MRI (MP-MRI) is accepted as the key imaging modality for the detection, localization and staging of prostate cancer. MP-MRI consists of  $T_2$  weighted imaging (T2WI) combined with at least one functional MR technique including diffusion-weighted imaging (DWI), dynamic contrast-enhanced imaging (DCEI) or spectroscopy. DWI is now most frequently used in clinical practice owing its high contrast resolution between tumour and benign tissue, its ability to quantitatively calculate parametric apparent diffusion coefficient (ADC) maps and the short acquisition time.<sup>3,4</sup>

MRI is the recommended modality for the local staging of prostate cancer. Differentiation between organ-confined disease (Stage T1–T2) and early advanced disease (Stage T3) has a profound impact on treatment decisions and patient prognosis.<sup>4,5</sup> Several studies in the literature on tumour detection, tumour localization and local tumour staging used 3.0-T scanners (higher cost than 1.5-T magnet) and an endorectal coil (increased cost and patient discomfort).<sup>6–8</sup> Some studies use an extended MRI examination, with T2WI in combination with multiple functional techniques (DWI  $\pm$  DCEI  $\pm$  spectroscopy).<sup>6,9</sup> This implies a relatively long acquisition time and increased cost (contrast agent).

The aim of this study was to evaluate the efficacy of a limited examination at 1.5-T MRI without endorectal coil for local prostate cancer staging (T stage) using anatomical  $T_2$  weighted MRI and diffusion-weighted MRI.

## METHODS AND MATERIALS

### Patients

This retrospective study was approved by the institutional ethical review board. The inclusion criteria were: (a) prostate MRI at 1.5T without endorectal coil, including  $T_1$  weighted image (T1WI), T2WI and DWI with  $b$ -values ranging from 0 to  $1000 \text{ s mm}^{-2}$  (B0, B50, B100, B500, B750 and B1000) performed between 1 May 2012 and 31 August 2014; and (b) radical prostatectomy performed within 6 months of MRI. Patient exclusion criteria were prior treatment (*e.g.* hormone therapy or radiotherapy) for prostate cancer ( $n = 5$ ), suboptimal quality of the prostatectomy specimen owing to capsule incision at the tumour site ( $n = 4$ ), prostate tumours invisible on MRI ( $n = 11$ ) and suboptimal quality of the MRI because of biopsy-related haemorrhage, artefacts of hip prosthesis and motion artefacts ( $n = 7$ ). The final study population thus consisted of 123 males. The clinical and pathological features of the study population are shown in Table 1.

### MRI protocol

MRI was performed on a 1.5-T magnet (Aera; Siemens Medical Systems, Erlangen, Germany) using a combination of an 18-channel phased-array body coil and 32-channel spine coil. Axial, coronal and sagittal  $T_2$  weighted turbo spin-echo MRI, axial  $T_1$  weighted turbo spin-echo MRI and axial echoplanar DWI with 6 different  $b$ -values (B0, B50, B100, B500, B750 and B1000) were obtained by covering the prostate gland and seminal vesicles. Axial T2WIs were obtained perpendicular to the

course of the prostatic urethra. Coronal images were obtained in the true coronal plane. The software package enabled an automated calculation of the ADC maps using the acquired  $b$ -values. The acquisition parameters for the T1WI, T2WI and DWI are summarized in Table 2. The total acquisition time was approximately 16 min.

### MR image evaluation

All MRI studies were evaluated retrospectively by three urologists with different levels of experience in prostate imaging, 25 years (RO), 15 years (LDW) and 3 years (EV), respectively. Images were evaluated at a digital workstation (Impax; Agfa, Mortsel, Belgium).

Local staging was performed based on the features described in the literature. The direct signs of extracapsular extension (ECE) were focal capsular irregularity/disruption, tumour signal intensity in the periprostatic fat, neurovascular bundle asymmetry or invasion and obliteration of the rectoprostatic angle. The indirect signs of ECE were capsular bulging and tumour contact length  $>20 \text{ mm}$  (Figure 1).<sup>4,10,11</sup> The presence of seminal vesicle invasion was based on the asymmetric low signal intensity within or along the lumen on T2WI and obliteration of the angle between the prostate and the seminal vesicle.<sup>4,12</sup> The following classification was used as the base of the analysis of the invasion pattern: Type I is directly spread into the seminal vesicles along the ejaculatory duct complex (Figure 2). Type II corresponds to direct tumour invasion of one or both seminal

Table 1. Clinical and pathological features

Characteristics	Study population ( $n = 123$ )
Age (years)	65.3 (49.3–77.7)
Prostate volume (ml)	38.7 (15–95)
Pre-operative PSA ( $\text{ng ml}^{-1}$ )	11.4 (1.4–200)
Clinical stage	
cT1	60 (48.8%)
cT2	51 (41.5%)
cT3–cT4	12 (9.8%)
Gleason score on surgical specimen	
6	22 (17.9%)
3+4 (7)	54 (43.9%)
4+3 (7)	20 (16.3%)
8	13 (10.6%)
9	14 (11.4%)
Histological tumour volume (ml)	4.8 (0.3–47.5)
D'Amico risk classification	
Low risk	15 (12.2%)
Medium risk	74 (60.2%)
High risk	34 (27.8%)

PSA, prostate-specific antigen.

Data are means (ranges) or counts (percentages).

Table 2. MRI acquisition protocol

Sequence	TR/ TE (ms)	Slice thickness (mm)	Matrix	FOV (mm)	Pixel size (mm)	Slices (number)	Scan time (min : s)
$T_2$ weighted TSE sagittal	7700/133	3.5	448 × 403	260 × 260	0.6 × 0.6	26	1 : 49
$T_2$ weighted TSE coronal	14010/124	3.5	448 × 403	260 × 260	0.6 × 0.6	40	2 : 50
$T_2$ weighted TSE axial	11250/124	3	448 × 365	260 × 236	0.6 × 0.6	56	5 : 05
DWI EPI axial	9900/67	4	128 × 104	350 × 285	2.7 × 2.7	42	5 : 47
$T_1$ weighted SPGR axial—fatsat	4.26/2.09	3.0	320 × 195	320 × 260	1.0 × 1.0	52	0 : 18

DWI, diffusion-weighted imaging; EPI, echoplanar imaging; fatsat, fat saturation; FOV, field of view; SPGR, spoiled gradient; TE, echo time; TR, repetition time; TSE, turbo spin echo.

vesicles through the prostatic capsule. Type III is defined as microscopic metastasis into the seminal vesicles without continuous spread.<sup>7,13</sup> Evaluation of the invasion of adjacent organs (T4) was performed with a high specificity level. T1WIs were obtained to exclude false-positive findings owing to biopsy-related haemorrhage. High-intensity areas on the T1WI matching low signal intensity on the T2WI were considered as haemorrhage.

#### Histopathological analysis

The prostate specimens were fixed overnight in 6% formaldehyde and coated with ink to allow proper orientation. Seminal

vesicles were separated from the prostate and examined separately. The prostate was weighed, measured and sliced from the apex to the base at 3-mm intervals perpendicular to the urethra for appropriate comparison with the MRI slices. Gleason score and pathological tumour stage were determined according to the TNM classification (*i.e.* extent of tumour (local), nodal and distant metastatic cancer burden). Absolute tumour volume was measured as follows: tumour volume (cubic centimetre) = [sum of all tumour areas on the slices (square centimetre) × slice thickness (0.3 cm) × 1.33 (shrinkage factor)]. In this study, the index or dominant tumour was correlated with the MRI study.

Figure 1. A 71-year-old patient with pre-operative 4.7 ng ml<sup>-1</sup> prostate-specific antigen. (a) Axial  $T_2$  image: a hypointense lesion in the right lateral peripheral zone with tumour contact length >20 mm [indirect sign of extracapsular extension (ECE)]; no direct signs of ECE were present. (b) The apparent diffusion coefficient map: the lesion demonstrated restricted diffusion (arrow); (c) the whole-gland microscopic prostatectomy specimen with Gleason 4 + 5 tumour with broad capsular contact and tumour volume of 3.9 ml (outlined); (d) microscopic examination (×50): multifocal limited invasion of tumour (stars) into the periprostatic fat (white arrow) through the capsule (black arrows). A, anterior; Li, left; P, posterior; Re, right.

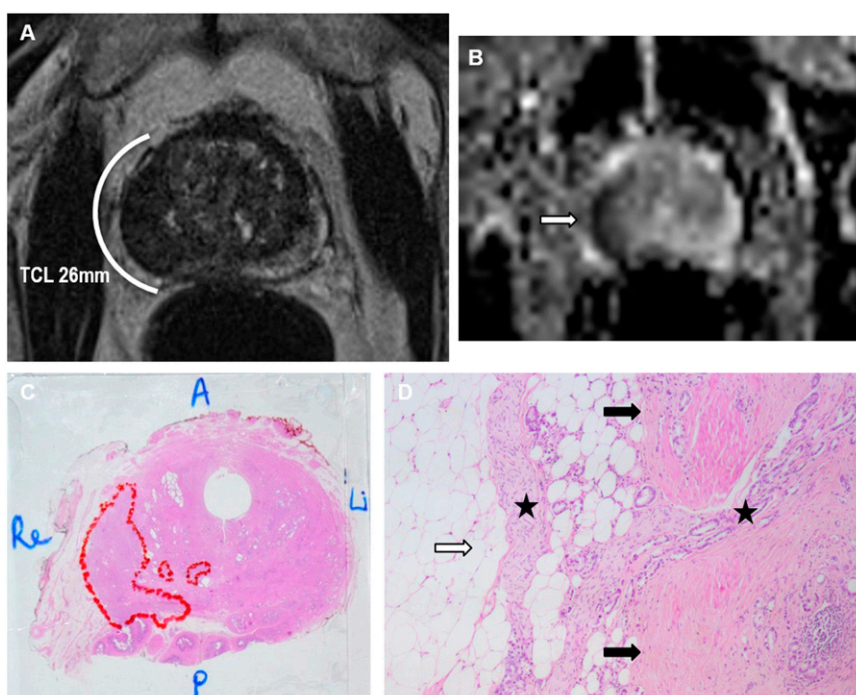
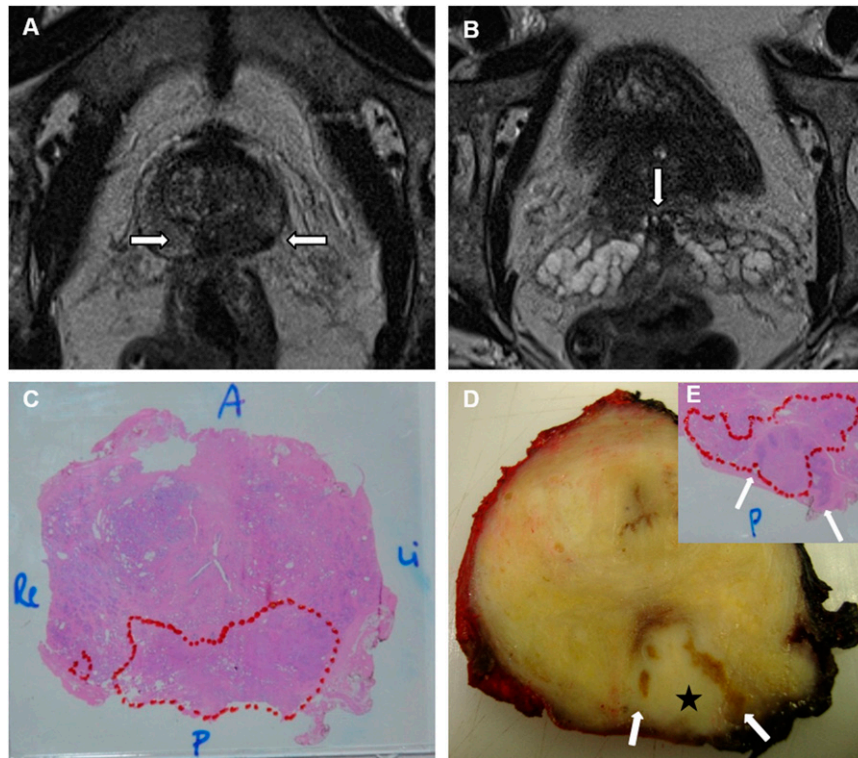


Figure 2. A 62-year-old patient with pre-operative  $5.1 \text{ ng ml}^{-1}$  prostate-specific antigen. (a) Axial  $T_2$  image: a hypointense lesion (arrows) in the posterior peripheral zone at the prostatic base (location of the ejaculatory duct complex); (b) axial  $T_2$  image: a subtle hypointense focus (arrow) in the left seminal vesicle root; (c) a whole-gland microscopic prostatectomy specimen, Gleason 4 + 3 tumour with broad capsular contact and tumour volume of 10.4 ml (outlined); (d, e) macroscopic and microscopic prostatectomy examination, tumour (star) invasion of the ejaculatory duct complex and the roots of the seminal vesicles (arrows). A, anterior; Li, left; P, posterior; Re, right.



The index tumour was defined in the following order of priority: (1) ECE; (2) Gleason score; and (3) tumour volume.<sup>14</sup> Tumour foci that were connected and with the same Gleason score were considered as one tumour.

#### Data correlation and statistical analysis

The findings on MRI were correlated with the histopathology by one radiologist (AVH) and one pathologist (AD). Correlation of MR images with histopathological sections remains challenging because of several procedural factors. First, the fixation and processing of the gland causes shrinkage and loss of volume. Also, the prostate may deform because of the loss of *in situ* position and fixation. Further, the slicing plane and slicing thickness of the MR images and the histopathological sections often show mismatch.<sup>6</sup>

For tumour staging, ECE (T3a) was considered correct if the predicted ECE on MRI was within 6 mm and was on the corresponding side. Further, seminal vesicle invasion (T3b) and invasion of adjacent structures (T4) were correlated. Sensitivity, specificity, positive and negative-predictive values and accuracy were calculated for different T stages.

#### RESULTS

The MRI performance for ECE is shown in Table 3. 61 patients of the study population had ECE of prostate cancer (T3a). When using direct signs only, the sensitivity was 57.4% and specificity

was 91.9%. When indirect signs were added to the direct signs, the sensitivity improved (85.2%) at the expense of moderate loss of specificity (83.9%). Of the 123 patients, 28 patients showed invasion of the seminal vesicles (T3b). The overall sensitivity for the detection of seminal vesicle invasion was low (53.6%). Analysis of the pattern of seminal vesicle involvement showed that Type I invasion was most frequently observed [19 (67.9%) patients] and only in 8 patients, invasion was detected on MR. Type II invasion was present in 8 (28.6%) patients and in 7 patients, invasion was correctly depicted on MR. Only one case showed microscopic Type III invasion not visible at MRI. The specificity, positive and negative-predictive values and accuracy were 98.9%, 93.8%, 87.9% and 88.6%, respectively. In nine patients, tumour extension to adjacent organs was present (T4), mainly invasion of the external sphincter (eight patients) (Figure 3). One patient had invasion of the bladder neck. In eight patients, adjacent organ invasion was correctly depicted on MRI. The sensitivity, specificity, positive and negative-predictive values and accuracy were 88.9%, 99.1%, 88.9%, 99.1% and 98.4%, respectively.

#### DISCUSSION

MP-MRI offers the most accurate imaging modality for local prostate cancer staging. However, data in published series on MRI staging performance are conflicting, and influencing factors include variation in acquisition protocols, magnetic field strength (3.0/1.5 T), use of an endorectal coil and reader



Table 3. MRI performance for extracapsular extension

Extracapsular extension	Sensitivity (%)	Specificity (%)	PPV (%)	NPV (%)	Accuracy (%)
Direct signs of T3a	57.4	91.9	87.5	68.7	74.8
Direct + indirect signs of T3a	85.2	83.9	83.9	85.2	84.6

NPV, negative-predictive value; PPV, positive-predictive value.

experience.<sup>15,16</sup> As MRI is increasingly being used in standard practice for local prostate cancer staging, the question rises whether a “limited” acquisition protocol would give acceptable results for appropriate patient care. In this study, prostate imaging was performed with a 1.5-T scanner without an endorectal coil and with only one functional MRI technique, *i.e.* DWI. This limited protocol obviously implicates loss of spatial resolution, functional information and probably staging performance. However, advantages are a relatively short acquisition time (approximately 16 min), cost reduction (no contrast agent and endorectal coil) and patient comfort (no endorectal coil). Nevertheless, such shortened MRI examinations could be beneficial with limited MR capacity.

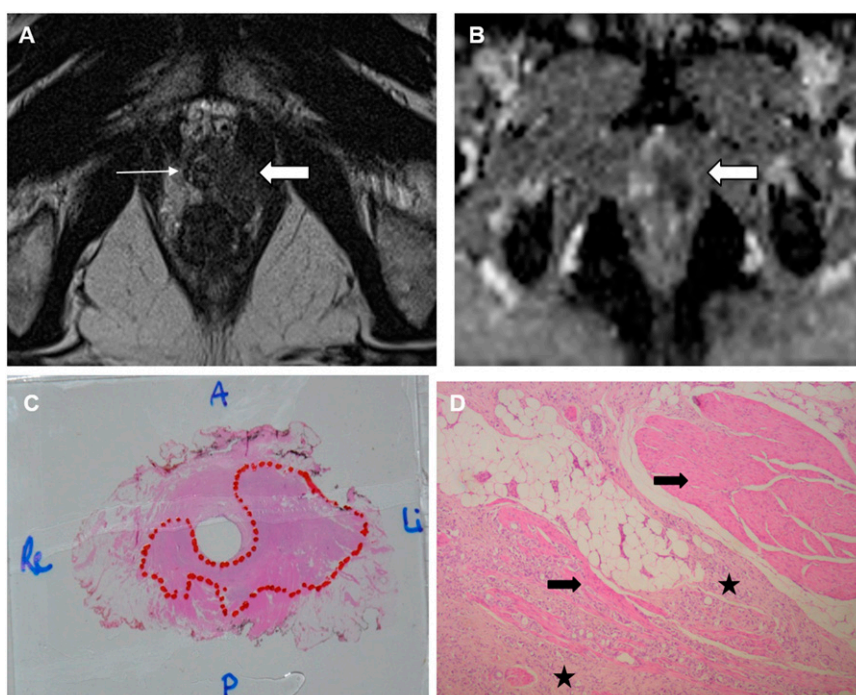
In our simplified multiparametric protocol, DWI was used as a functional MRI technique because it is fast, simple and readily available. Despite the low spatial resolution of DWI, studies have shown its potential role in predicting ECE.<sup>17,18</sup> The study of Woo et al<sup>18</sup> concluded that T2WI and DWI were independently associated with ECE and ADC had an incremental value in

patients without a high suspicion of ECE on T2WI. The role of DWI in seminal vesicle invasion has also been investigated. Kim et al<sup>19</sup> showed that the use of T2WI with DWI was more specific and accurate than T2WI alone for the prediction of seminal vesicle invasion.

Distinction between organ-confined disease (T2) and early extraprostatic disease (T3a) is crucial for treatment decisions and patient prognosis because <5% of patients demonstrate nodal metastases in T2 stage, as opposed to 15–30% in T3 stage.<sup>20</sup>

The studies of Fütterer et al<sup>7</sup> and Heijmink et al<sup>18</sup> yielded a high sensitivity (88% and 80%, respectively), very high specificity (96% and 100%, respectively) and high accuracy (94% and 93% respectively) for detecting ECE. Both studies used direct signs of ECE, a 3.0-T magnet and an endorectal coil. In our study, the sensitivity for ECE was relatively low using direct signs of ECE (57.4%), probably owing to the poor performance of MRI in detecting limited ECE (<1 mm), caused by limited spatial resolution. Therefore, indirect signs of ECE have been

Figure 3. A 62-year-old patient with pre-operative 95 ng ml<sup>-1</sup> prostate-specific antigen. (a) Axial T<sub>2</sub> image: a hypointense lesion (thick arrow) in the left peripheral zone at the prostatic apex with suspected invasion of the external sphincter on the left side (thin arrow). (b) The apparent diffusion coefficient map: the lesion demonstrated restricted diffusion (arrow); (c) a whole-gland microscopic prostatectomy specimen, Gleason 4 + 4 tumour in the prostate apex and tumour volume of 14 ml (outlined); (d) microscopic examination (×50): multifocal invasion of the tumour (stars) into the muscle fibres of the external sphincter (arrows). A, anterior; Li, left; P, posterior; Re, right.



described in the literature.<sup>10,11</sup> In our study, increase of sensitivity (57.4–83.9%) was achieved using the combination of direct and indirect signs. Nevertheless, the increase of sensitivity is at the expense of moderate loss of specificity (91.9–83.9%). Cornud et al<sup>10</sup> and Somford et al<sup>21</sup> postulated that either a high sensitivity reading or high specificity reading could be used according to the D'Amico risk classification. In low-risk prostate cancer (prostate-specific antigen  $\leq 10$  ng ml<sup>-1</sup>, Gleason score  $\leq 6$  and clinical Stage T1–T2a), a high sensitivity reading could be favoured to select optimal candidates for active surveillance or nerve-sparing radical prostatectomy, thereby avoiding underestimation of the disease. The use of indirect signs of ECE may also reduce the number of positive surgical margins. In high-risk prostate cancer (prostate-specific antigen  $> 20$  ng ml<sup>-1</sup>, Gleason score  $\geq 8$  and clinical Stage  $> T2c$ ), a high specificity reading could be beneficial to prevent incorrectly ruling out patients for potentially curative surgery on the basis of false-positive MRI results. However, in current clinical practice, extraprostatic disease is not (always) a contraindication for curative surgery. An advantage of a high specificity reading is the avoidance of unnecessary resection of the neurovascular bundle.<sup>10,21</sup>

The present study showed a low sensitivity and high specificity for the detection of seminal vesicle invasion (53.6% and 98.9%, respectively). Several other authors reported similarly a low sensitivity, ranging from 27% (with specificity of 95% in a meta-analysis of Engelbrecht et al<sup>22</sup>) to 59%.<sup>13,23</sup> However, sensitivity seems to be largely dependent on the pattern of tumour extension. Less than half of the cases of Type I invasion were depicted on MR (8/19 cases), because limited and/or microscopic invasion of the seminal vesicle root along the ejaculatory

duct complex remained undetectable. MR performed better in Type II invasion, as most of these tumours clearly invaded the seminal vesicle through the prostate capsule (8/9 cases).

Evaluating the MR staging performance of Stage T4 is difficult, because surgery is relatively a contraindication in these patients. In this study, ultimately 9 patients with invasion of adjacent organs were included and in 8 patients, invasion was correctly depicted on MR, yielding a sensitivity and specificity of 88.9% and 99.1%, respectively.

Limitations of this study include its retrospective design and relatively small study population, in particular for Stage T3b (28 cases) and Stage T4 (9 cases). Further, patients were not stratified according to D'Amico risk classification for the staging performance of ECE. We acknowledge that MR staging performance could be higher with an extensive acquisition protocol (DWI, DCEI and spectroscopy) and more advanced equipment (a 3.0-T scanner with endorectal coil). However, the aim of the study was to evaluate the efficacy of a limited acquisition protocol.

In conclusion, 1.5-T MRI without an endorectal coil and with limited acquisition protocol (T2WI, T1WI and DWI) provides a relatively high sensitivity for detecting Stage T3a when using the combination of indirect and direct signs of ECE (T3a). The sensitivity almost reaches the results of studies with a 3.0-T scanner and endorectal coil.<sup>7,8</sup> However, this high sensitivity reading is at the cost of a moderate loss of specificity. Invasion of the seminal vesicles (T3b) occurs most often along the ejaculatory duct complex with low MR sensitivity, in line with other published data.<sup>13,22,23</sup>

## REFERENCES

- Global Burden of Disease Cancer Collaboration; Fitzmaurice C, Dicker D, Pain A, Hamavid H, Moradi-Lakeh M, MacIntyre MF, et al. The global burden of cancer 2013. *JAMA Oncol* 2015; **1**: 505–27. doi: <http://dx.doi.org/10.1001/jamaoncol.2015.0735>
- Siegel RL, Miller KD, Jemal A. Cancer Statistics, 2015. *CA Cancer J Clin* 2015; **65**: 5–29. doi: <http://dx.doi.org/10.3322/caac.21254>
- Jung SI, Donati OF, Vargas HA, Goldman D, Hricak H, Akin O. Transition zone prostate cancer: incremental value of diffusion-weighted endorectal MR imaging in tumor detection and assessment of aggressiveness. *Radiology* 2013; **269**: 493–503. doi: <http://dx.doi.org/10.1148/radiol.13130029>
- Bonekamp D, Jacobs MA, El-Khouli R, Stoianovici D, Macura KJ. Advancements in MR imaging of the prostate: from diagnosis to interventions. *Radiographics* 2011; **31**: 677–703. doi: <http://dx.doi.org/10.1148/rg.313105139>
- Heidenreich A, Bastian PJ, Bellmunt J, Bolla M, Joniau S, van der Kwast T, et al. EAU guidelines on prostate cancer. Part 1: screening, diagnosis, and local treatment with curative intent—update 2013. *Eur Urol* 2014; **65**: 124–37. doi: <http://dx.doi.org/10.1016/j.eururo.2013.09.046>
- Turkbey B, Pinto PA, Mani H, Bernardo M, Pang Y, McKinney YL, et al. Prostate cancer: value of multiparametric MR imaging at 3 T for detection-histopathologic correlation. *Radiology* 2010; **255**: 89–99. doi: <http://dx.doi.org/10.1148/radiol.09090475>
- Fütterer JJ, Heijmink SW, Scheenen TW, Jager GJ, Hulsbergen-Van de Kaa CA, Witjes JA, et al. Prostate cancer: local staging at 3-T endorectal MR imaging—early experience. *Radiology* 2006; **238**: 184–91. doi: <http://dx.doi.org/10.1148/radiol.2381041832>
- Heijmink SW, Fütterer JJ, Hambrock T, Takahashi S, Scheenen TW, Huisman HJ, et al. Prostate cancer: body-array versus endorectal coil MR imaging at 3 T—comparison of image quality, localization, and staging performance. *Radiology* 2007; **244**: 184–95. doi: <http://dx.doi.org/10.1148/radiol.2441060425>
- Fütterer JJ, Heijmink SW, Scheenen TW, Veltman J, Huisman HJ, Vos P, et al. Prostate cancer localization with dynamic contrast-enhanced MR imaging and proton MR spectroscopic imaging. *Radiology* 2006; **241**: 449–58. doi: <http://dx.doi.org/10.1148/radiol.2412051866>
- Cornud F, Rouanne M, Beuvon F, Eiss D, Flam T, Liberatore M, et al. Endorectal 3D T2-weighted 1 mm-slice thickness MRI for prostate cancer staging at 1.5 Tesla: Should we reconsider the indirect signs of extracapsular extension according to the D'Amico tumor risk criteria. *Eur J Radiol* 2012; **81**: e591–7. doi: <http://dx.doi.org/10.1016/j.ejrad.2011.06.056>

11. Baco E, Rud E, Vlatkovic L, Svindland A, Eggesbø HB, Hung AJ, et al. Predictive value of magnetic resonance imaging determined tumor contact length for extracapsular extension of prostate cancer. *J Urol* 2015; **193**: 466–72. doi: <http://dx.doi.org/10.1016/j.juro.2014.08.084>
12. Roethke M, Kaufmann S, Kniess M, Ketelsen D, Claussen CD, Schlemmer HP, et al. Seminal vesicle invasion: accuracy and analysis of infiltration patterns with high-spatial resolution T2-weighted sequences on endorectal magnetic resonance imaging. *Urol Int* 2014; **92**: 294–9. doi: <http://dx.doi.org/10.1159/000353968>
13. Ohori M, Scardino PT, Lapin SL, Seale-Hawkins C, Link J, Wheeler TM. The mechanisms and prognostic significance of seminal vesicle involvement by prostate cancer. *Am J Surg Pathol* 1993; **17**: 1252–61. doi: <http://dx.doi.org/10.1097/00000478-199312000-00006>
14. van der Kwast TH, Amin MB, Billis A, Epstein JI, Griffiths D, Humphrey PA, et al; ISUP Prostate Cancer Group. International Society of Urological Pathology (ISUP) consensus conference on handling and staging of radical prostatectomy specimens. Working group 2: T2 substaging and prostate cancer volume. *Mod Pathol* 2011; **24**: 16–25. doi: <http://dx.doi.org/10.1038/modpathol.2010.156>
15. Murphy G, Haider M, Ghai S, Sreeharsha B. The expanding role of MRI in prostate cancer. *AJR Am J Roentgenol* 2013; **201**: 1229–38. doi: <http://dx.doi.org/10.2214/AJR.12.10178>
16. Soylu FN, Eggner S, Oto A. Local staging of prostate cancer with MRI. *Diagn Interv Radiol* 2012; **18**: 365–73. doi: <http://dx.doi.org/10.4261/1305-3825.DIR.4970-11.2>
17. Kim CK, Park SY, Park JJ, Park BK. Diffusion-weighted MRI as a predictor of extracapsular extension in prostate cancer. *AJR Am J Roentgenol* 2014; **202**: W270–6. doi: <http://dx.doi.org/10.2214/AJR.13.11333>
18. Woo S, Cho JY, Kim SY, Kim SH. Extracapsular extension in prostate cancer: added value of diffusion-weighted MRI in patients with equivocal findings on T2-weighted imaging. *AJR Am J Roentgenol* 2015; **204**: W168–75. doi: <http://dx.doi.org/10.2214/AJR.14.12939>
19. Kim CK, Choi D, Park BK, Kwon GY, Lim HK. Diffusion-weighted MR imaging for the evaluation of seminal vesicle invasion in prostate cancer: initial results. *J Magn Reson Imaging* 2008; **28**: 963–9. doi: <http://dx.doi.org/10.1002/jmri.21531>
20. Paño B, Sebastià C, Buñesch L, Mestres J, Salvador R, Macías NG, et al. Pathways of lymphatic spread in male urogenital pelvic malignancies. *Radiographics* 2011; **31**: 135–60. doi: <http://dx.doi.org/10.1148/rgr.311105072>
21. Somford DM, Hamoen EH, Fütterer JJ, van Basten JP, Hulsbergen-van de Kaa CA, Vreuls W, et al. The predictive value of endorectal 3 Tesla multiparametric magnetic resonance imaging for extraprostatic extension in patients with low, intermediate and high risk prostate cancer. *J Urol* 2013; **190**: 1728–34. doi: <http://dx.doi.org/10.1016/j.juro.2013.05.021>
22. Engelbrecht MR, Jager GJ, Laheij RJ, Verbeek AL, van Lier HJ, Barentsz JO. Local staging of prostate cancer using magnetic resonance imaging: a meta-analysis. *Eur Radiol* 2002; **12**: 2294–302. doi: <http://dx.doi.org/10.1007/s00330-002-1389-z>
23. Soylu FN, Peng Y, Jiang Y, Wang S, Schmid-Tannwald C, Sethi I, et al. Seminal vesicle invasion in prostate cancer: evaluation by using multiparametric endorectal MR imaging. *Radiology* 2013; **267**: 797–806. doi: <http://dx.doi.org/10.1148/radiol.13121319>